Electronics Letters

AN INTERNATIONAL PUBLICATION

LIBRARY COPY

CONTENTS

8th AUGUST 1974 Vol. 10 No. 16

pages 329–348

THE INSTITUTION OF ELECTRICAL ENGINEERS

barrier profiling technique varied between about 2.4×10^{13} cm^{-3} at the surface to a minimum of about 1.9×10^{12} cm^{-3} before the n^+ substrate.

For the time-of-flight technique, Schottky barriers were made by the evaporation of gold dots of 412 μm diameter and 1600 Å thickness on the GaAs surface, which had been previously etched with bromine–methanol. Pulses of 22 keV electrons of about 40 ps duration were used to bombard the Schottky barrier and create the secondary bunch in the semiconductor surface. These pulses were produced by an electron microscope fitted with a deflection system similar to that described by Sigmon *et al.*[2] The number of secondaries was about 7×10^5, and they gave a negligible perturbation of the electric field in the samples. The samples were reverse biased by a stripline bias T, and the current pulses due to the electron-bunch transits were detected by a sampling oscilloscope with a risetime of 25 ps. The risetime of the detected current pulse was limited by the sample capacitance, and was about 150 ps.

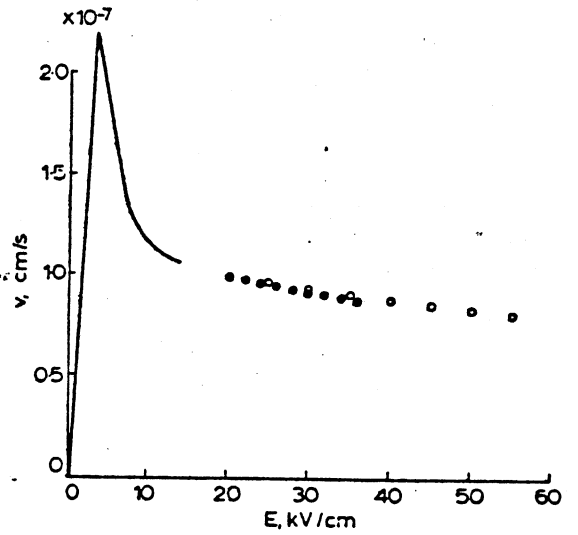

Fig. 2 *Velocity/field characteristic for electrons in GaAs*
○ measured on sample 1
● measured on sample 2
— Ruch and Kino[1]

Fig. 1 shows τ against V for both samples for the experiment carried out at 300 K. The constants A and B were determined for each sample and used to calculate the points for the $v(E)$ characteristics, which are shown in Fig. 2. The $v(E)$ characteristics are seen to be in good agreement for both samples. The transit current pulses were flat topped for the highest voltages used and showed no evidence of avalanche multiplication or trapping effects. The low field mobility of the samples was about 8200 $cm^2 V^{-1} s^{-1}$, as this mobility was measured by the Van der Pauw technique on a similar layer grown on a semi-insulating substrate. The part of the $v(E)$ characteristic measured by Ruch and Kino,[1] also by the time-of-flight technique and on good high mobility material, is shown in Fig. 2. The curves match reasonably well.

Acknowledgment: We are grateful to P. D. Greene of STL, Harlow, for supplying the GaAs samples.

P. A. HOUSTON
A. G. R. EVANS

Department of Natural Philosophy
University of Strathclyde
107 Rottenrow, Glasgow G4 ONG, Scotland

1st July 1974

References

1 RUCH, J. G., and KINO, G. S.: 'Transport properties of GaAs', *Phys. Rev.*, 1968, 174, pp. 921–931
2 SIGMON, T. W., GIBBONS, J. F., and NORRIS, C. B.: 'Observation of localised radiation damage in silicon', *Appl. Phys. Lett.*, 1969, 14, pp. 90–92

SYNTHESIS OF TRANSFER FUNCTIONS BY SIGNAL-FLOW GRAPHS

Indexing terms: Linear network synthesis, Transfer functions

A new procedure is given for the synthesis of voltage transfer functions. It is shown that the well known circuits of Lovering and Brugler can also be derived easily by this method. It is also indicated that a simplification can be obtained in the *RC*:–*RC* decomposition method, which is in the proposed procedure.

Introduction: Lovering[1] has analysed a special *RC* circuit configuration and has shown that a general voltage transfer function can be brought into a form through *RC*:–*RC* decomposition so that the admittance functions of simple *RC* circuits in the configuration can be easily identified. Brugler[2] has considered a different *RC* network configuration, and has shown that a general voltage transfer function can be realised by this network. However, to put the given transfer function into the desired form, a condition between various admittances must be satisfied. The use of signal-flow graphs in the synthesis of active *RC* networks appears to be more promising, as described in References 3 and 4. However, the method given in Reference 3 becomes more difficult to apply when the order of the transfer function increases. The method given in Reference 4 requires lengthy and time-consuming manipulations, and also the element values are obtained from a set of equations with some restrictions. The synthesis procedure used by Anday[5] uses a new signal-flow-graph representation for the biquadratic transfer functions. This method, which is an alternative approach to state-variable realisation,[3] is based on drawing the signal-flow graph directly from the given transfer function and obtaining the active circuit from this graph. In this letter, a new procedure for deriving the circuits given by Lovering and Brugler is obtained by a new signal-flow-graph representation of the voltage transfer functions. The procedure provides a means of generating new network configurations for the same transfer functions. One such new network is given in this letter. Also, a rule is given that reduces the number of passive elements in the active network to be realised by *RC*:—*RC* decomposition.

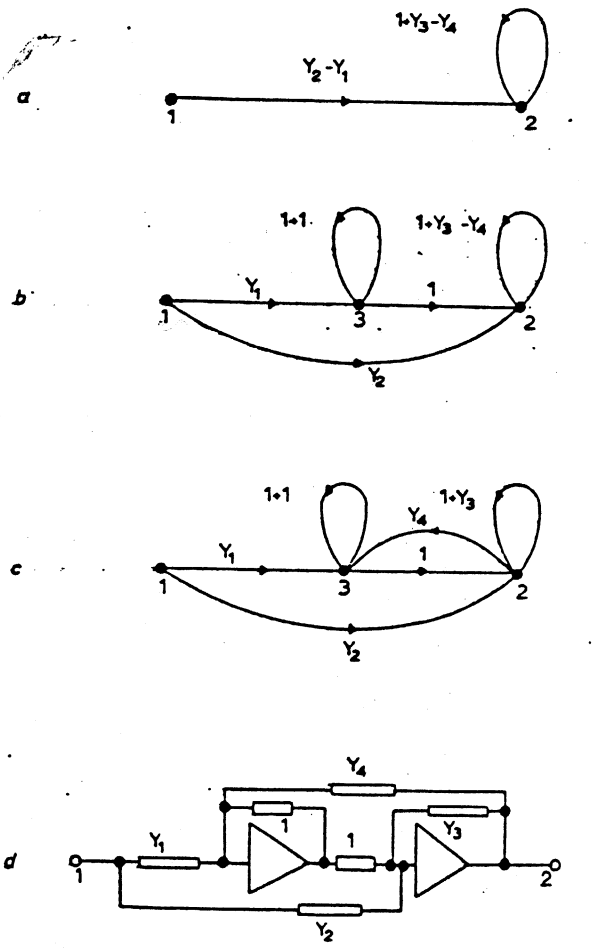

Fig. 1 *Realisation of nth-order transfer functions by Lovering's configuration*

Realisation: Consider the nth-order transfer function

$$T(s) = \frac{V_2}{V_1} = \frac{N(s)}{D(s)} \quad \ldots \quad (1)$$

By RC:–RC decomposition, it can be put in the form

$$T(s) = \frac{Y_1 - Y_2}{Y_3 - Y_4} \quad \ldots \quad (2)$$

where Y_1, Y_2, Y_3 and Y_4 are admittance functions. From eqns. 1 and 2, we have

$$V_1(Y_2 - Y_1) + V_2(1 + Y_3 - Y_4) = V_2 \quad \ldots \quad (3)$$

The signal-flow graph for eqn. 3 is shown in Fig. 1*a*. Applying the well known transformation rules indicated in Figs. 1*b* and*c*, a realisable signal-flow graph[5] shown in Fig. 1*c* is obtained. The corresponding circuit realisation is the one given by Lovering, and is shown in Fig. 1*d*. On the other hand, if eqn. 3 is written in the following form:

$$V_1\left(\frac{Y_1}{Y_1+Y_4+Y_5} - \frac{Y_2}{Y_2+Y_3+Y_6}\right) + V_2\left(1 + \frac{Y_4}{Y_1+Y_4+Y_5} - \frac{Y_3}{Y_2+Y_3+Y_6}\right) = V_2 \quad (4)$$

where the admittances satisfy the relation

$$Y_1 + Y_4 + Y_5 = Y_2 + Y_3 + Y_6$$

a signal-flow graph corresponding to eqn. 4 is drawn and transformed to the realisable form.[6] Thus we easily obtain Brugler's circuit configuration. Now, if eqn. 3 is written as

$$V_1(Y_1 - Y_2) + V_2(1 + Y_4 - Y_3) = V_2 \quad \ldots \quad (5)$$

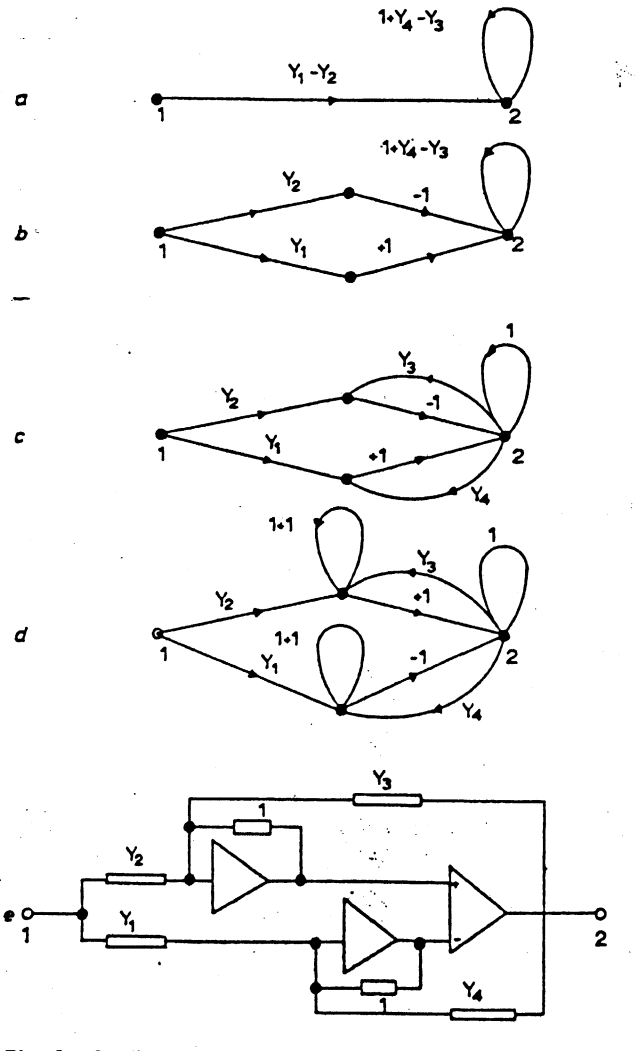

Fig. 2 *Realisation of nth-order transfer function by new configuration*

the corresponding signal-flow in Fig. 2*a* is obtained. Applying the well known transformation rules indicated in Figs. 2*b*, *c* and *d*, a realisable signal-flow graph[6] is obtained. Its circuit realisation corresponds to a new circuit as shown in Fig. 2*e*.

Some simplifications in the RC:–RC decomposition: In general, the polynomials in eqn. 1 are of the form

$$\left.\begin{aligned} N(s) &= (b_{m-k}s^{m-k} + \ldots + b_0)\prod_{i=1}^{k}(s+\sigma_{iz}) \quad \sigma_{iz} \geq 0 \\ \text{and} \\ D(s) &= (a_{n-l}s^{n-l} + \ldots + a_0)\prod_{i=1}^{l}(s+\sigma_{ip}) \quad \sigma_{ip} \geq 0 \end{aligned}\right\} \quad \ldots \quad (6)$$

The passive elements of the circuits shown in Figs. 1*d* and 2*e* are made of simple RC admittance functions and two resistances of 1Ω. If we select $A(s)$ to be an arbitrary polynomial for RC:–RC decomposition:

(*a*) $A(s) = \prod^{k}(s+\sigma_{iz})\prod^{l}(s+\sigma_{ip})\prod^{t}(s+\sigma_{ia}) \quad k+l < n-1$

(*b*) $A(s) = \prod^{k}(s+\sigma_{iz})\prod^{l}(s+\sigma_{ip}) \quad k+l = n-1$

(*c*) $A(s) = \prod^{k_0}(s+\sigma_{iz})\prod^{l_0}(s+\sigma_{ip})\ k_0+l_0 = n-1,\ k+l > n-1$

it can be shown that the number of passive elements n_p is given by

$$n_p = 4n+2-2(K+L) \quad K+L \leq n-1 \quad \ldots \quad (7)$$

where K and L are the number of distinct zeros and poles, respectively, of $T(s)$ on the negative real axis. If, in the decomposition, the above rule is neglected, the number of passive elements in the circuit becomes $n_p = 4n+2$; therefore $2(K+L)$ more passive elements are to be used.

Example: Given

$$T(s) = \frac{N(s)}{D(s)} = \frac{(s+4)(s^2+s+1)}{(s+3)(s^2+3s+1)}$$

(i) Following the rule if $A(s)$ is $A(s) = (s+3)(s+4)$, we have

$$\frac{N(s)}{A(s)} = \frac{s^2+s+1}{s+3} = \tfrac{1}{3} + s - \frac{7/3\,s}{s+3}$$

and

$$\frac{D(s)}{A(s)} = \frac{s^2+3s+1}{s+4} = \tfrac{1}{4} + s - \frac{5/4\,s}{s+4}$$

and $n_p = 10$

(ii) If the proposed rule is not considered and the polynomial $A(s)$ is $A(s) = (s+1)(s+2)$, we have

$$\frac{N(s)}{A(s)} = \frac{(s+4)(s^2+s+1)}{(s+1)(s+2)} = 2 + s + \frac{3s}{s+2} - \frac{3s}{s+1}$$

and

$$\frac{D(s)}{A(s)} = \frac{(s+3)(s^2+3s+1)}{(s+1)(s+2)} = \tfrac{3}{2} + s + \frac{2s}{s+1} - \frac{\frac{1}{2}s}{s+2}$$

and $n_p = 14$.

Acknowledgment: The author wishes to thank Prof. Y. Tokad for his valuable suggestions.

S. CAN

Technical University of Istanbul
Engineering & Architecture Faculty
Electrical Engineering Department
Beşiktaş-Istanbul, Turkey

8th July 1974

References

1 LOVERING, W. F.: 'Analog computer simulation of transfer functions', *Proc. Inst. Elec. Electron. Eng.*, 1965, 53, pp. 306–307
2 BRUGLER, J. S.: '*RC* synthesis with differential-input operational amplifiers' *in* NEWCOMB, R. W., and RAO, T. (Eds.): 'Papers on integrated circuit synthesis'. Stanford University Centre for Systems Research Technical Report 6560–4, 1966, pp. 115–130

3 KERWIN, W. J. HUELSMAN, L. P. and NEWCOMB, R. W.: 'State-variable synthesis for insensitive integrated circuit transfer functions', *IEEE J. Solid-State Circuits*, 1967, SC-2, pp. 87–92
4 ROBINSON, A. E., and METHIWALA, A. K.: 'Method for generating low-sensitivity *RC* active circuits', *Electron Lett.*, 1970, 6, pp. 95–96
5 ANDAY, F.: 'Alternate state-variable realizations using single-ended operational amplifiers', *Proc. Inst. Elect. Electron. Eng.*, 1971, 59, pp. 1710–1711
6 ANDAY, F.: 'Realization of transfer function using differential-input operational amplifier', *ibid.*, 1972, 60, pp. 445–446

PREPARATION OF WATER-FREE SILICA-BASED OPTICAL-FIBRE WAVEGUIDE

Indexing terms: Fibre optics, Light absorption, Losses, Optical waveguides

A technique is described whereby the hydroxyl absorption bands of the new phosphosilicate-core optical-fibre waveguide, which arise from impurities in the cladding, can be largely eliminated. The resulting fibre has ultralow loss over the entire wavelength range 0·4–1·1 μm.

Introduction: A problem commonly encountered in the preparation silica-based optical fibres is the presence of OH absorption bands at a number of wavelengths,[1-5] particularly at 0·95 μm. We have observed the same effect in a new type of fibre[6,7] comprising a phosphosilicate glass core in a silica cladding. These fibres are made by an accurately controlled chemical-vapour-deposition technique in which silicon tetrachloride and phosphorus oxychloride are simultaneously oxidised and fused into a clear layer of phosphosilicate glass on the inside of a silica tube that is subsequently drawn into a fibre.

It is found that, when the silica tubing used is of a synthetic grade of high hydroxyl content (1200 parts in 10^6), such as Suprasil, the minimum attenuation is between 2 and 3 dB/km, and the OH band at 0·95 μm rises to a peak of about 40 dB/km. On the other hand, with Heralux tubing, in which the water concentration is only one-tenth that in Suprasil, but the level of other impurities is higher, the minimum loss rises to 6 dB/km, but the peak at 0·95 μm falls to 15 dB/km. This is a strong indication that the cladding has an appreciable effect on the transmission loss, which is to be expected, since, at the normalised frequency of the fibre of $V = 20$, it carries approximately 10% of the propagating power. We conclude, therefore, that the OH impurity giving rise to the absorption bands is present mainly in the cladding and not in the vapour-deposited core. It follows that, if the relative amount of optical power propagating in the impure cladding can be decreased, the hydroxyl bands can be correspondingly reduced.

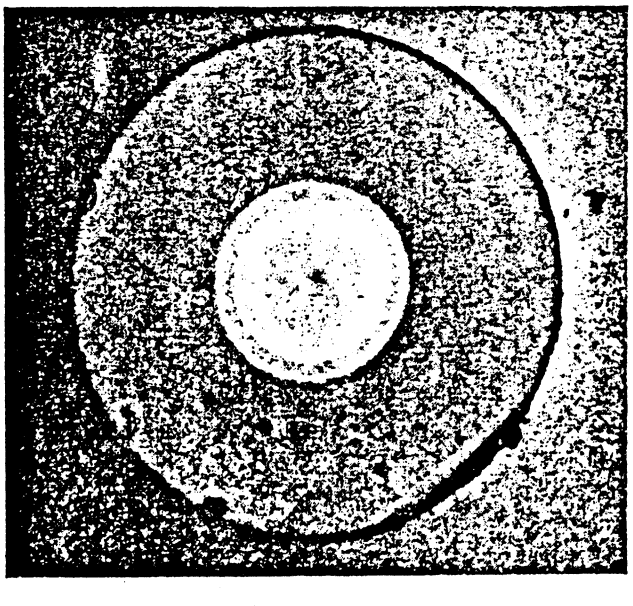

Fig. 1 *Cross-section of stepped-refractive-index fibre*
Showing the Suprasil cladding and three successive core layers of increasing refractive index. The overall diameter is 145 μm

Method: One method of doing this during the preparation of the phosphosilicate-core fibre would be to deposit initially a silica layer of low hydroxyl content on the inside of the commercial silica supporting tube. This can be done, but, to produce simultaneous oxidation and fusion to a clear glassy layer, the deposition rate must be kept low. Thus the time taken to build up the required thickness of this layer is unnecessarily long. However, if, instead, a layer of phosphosilicate glass having a suitably small proportion of P_2O_5 is deposited, the deposition rate can be increased appreciably, and the refractive index is not changed greatly from that of silica.

An alternative approach is to use the fact that a graded-refractive-index core effectively restricts the optical power to a region closer to the fibre axis than in a normal cladded fibre. Reflections at the core–cladding interface do not occur, except for those rays propagating near the critical angle, and hence the amount of power contained in the cladding is reduced. With our method of vapour deposition, the fabrication technique for a graded-refractive-index fibre is a simple one and involves only successive changes in the relative concentration of the reacting gases. The first layer may now, as before, contain a suitably small proportion of P_2O_5 and may be deposited at a much higher rate than the silica. The second, and subsequent, layers contain increasing concentrations. The total deposition time for the entire core is about 1 h. However, we have found that a stepped approximation to a graded-refractive-index core, in which the refractive index increases in three successive steps, is equally effective in confining the optical power to the core region. We have fabricated fibres of all three types, but present here the results obtained only for the latter version.

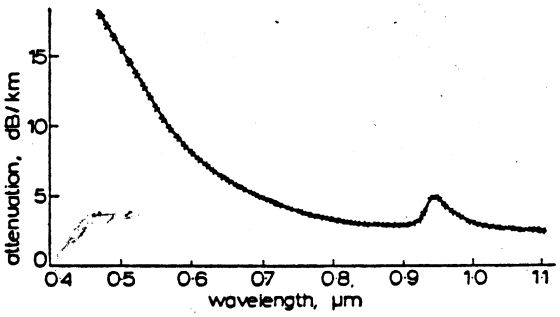

Fig. 2 *Spectral attenuation curve of 1·2 km length of phosphosilicate-core silica-cladded fibre shown in Fig. 1*

Results and discussion: A typical fibre cross-section (Fig. 1) clearly shows the Suprasil cladding and the three layers of increasing refractive index. The overall diameter is 145 μm and the numerical aperture of this particular fibre is 0·16. The spectral attenuation has been measured over the entire drawn length of 1·2 km and the resulting curve (Fig. 2) is remarkably smooth. As predicted,[7] the broad iron absorption band in the vicinity of 1 μm has been largely removed by some fairly straightforward improvements in fabrication techniques. Further, the intermediate layers have almost eliminated all the OH bands. The only one remaining is that at 0·95 μm, but its height has been reduced to 2 dB/km. In fact, in some other samples, the magnitude is only 0·8 dB/km and the effect of the wings of the band at the semiconductor-laser wavelength is negligible. As a result of these modifications, the attenuation is very low over the entire wavelength range and is below 5 dB/km between 0·7 μm and the highest wavelength measured (1·1 μm) with a minimum of 2·4 dB/km. Even at 0·45 μm, the loss is less than 20 dB/km and transmission in the near ultraviolet, in particular, is considerably better than has previously been reported[8] for conventional u.v.-transmitting fibres. It should be noted that extrapolated absorption and scatter measurements suggest that, at least from 0·4 to 1·1 μm, the intrinsic loss of phosphosilicate glass is similar to that of pure silica. This indicates that, with further improvements, it should be possible to obtain an attenuation of less than 2 dB/km in the régime (from 0·85 to 0·9 μm) of gallium-arsenide devices, and still lower values at longer wavelengths. Measurements